

Drag Measurement in Flows of 50 Microsecond Duration

A.L. Smith and D.J. Mee

Department of Mechanical Engineering
The University of Queensland
Brisbane QLD 4072, AUSTRALIA

Abstract

This paper describes the extension of the stress wave force balance first proposed by Sanderson [1] to flows in an expansion tube where test times may be as short as 50 μ s. The technique is first demonstrated for a 30° semi-angle sharp cone by comparing the forces measured with those expected theoretically. Agreement to within 5% is achieved. Two re-entry heat shields were then tested in a Carbon Dioxide test flow where the flow velocity was in excess of 7000 ms^{-1} . The experimental drag forces agreed with those obtained from a Modified-Newtonian prediction to within 11%.

1 Introduction

Wind tunnel testing of flight vehicles has been important in the development of new designs. Measurement of overall forces on vehicles is necessary to determine the performance of control surfaces and is usually one of the primary goals of an experimental programme.

Hypervelocity impulse facilities, such as shock tunnels and expansion tubes, are capable of producing flows representative of the re-entry of vehicles at near orbital velocities. However, the impulsive nature of these facilities restricts the steady test flow period. These may be as short as 1 ms for shock tunnels and 50 μ s for expansion tubes. Consequently, traditional force measurement techniques cannot be employed as there is insufficient time for the model and its support to reach static equilibrium.

This paper addresses the measurement of drag in impulse facilities where the test time is approximately 50 μ s. One of the applications of such a measurement capability is in the studies of the re-entry of vehicles into the Martian atmosphere (which is primarily Carbon Dioxide). The results from drag measurements on re-entry type models in a small expansion tube with Carbon Dioxide as the test gas is detailed.

2 Experimental Facility

The experiments were conducted in the X1 facility located at The University of Queensland (Neely *et al.* [2]). This facility was originally designed as a reflected shock tunnel but has been adapted to investigate the mating of a free piston driver with an expansion tube. The X1 facility is shown schematically in Figure 1.

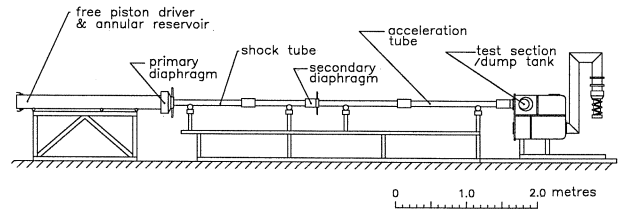


Figure 1: Layout of X1 facility.

The free piston driver uses a 3.4 kg piston which is contained within the compression tube. The compression tube has an internal diameter of 100 mm and is 2300 mm in length. Both the shock and acceleration tubes have internal diameters of 37 mm and are 2080 mm and 2940 mm in length, respectively.

The facility was operated as a free piston driven expansion tube using Carbon Dioxide as the test gas. The test condition produced approximately 50 μ s of steady test flow. The typical filling pressures and test flow conditions, along with their respective uncertainties, are listed in Table 1.

Table 1: Typical fill pressures and test conditions for the X1 facility.

Condition	1	
Operating Mode	Expansion Tube	
Driver gas	80% He	20% Ar
Test gas	CO ₂	
Acceleration gas	He	
Fill Pressures		
Compression tube (kPa)	78 He	17 Ar
Shock Tube (kPa)	5	
Acceleration tube (Pa)	100	
Test Flow		
Shock velocity (ms^{-1})	7200	$\pm 3.0\%$
Test velocity (ms^{-1})	7200 ¹	$\pm 3.0\%$
Static pressure (kPa)	15.6	$\pm 3.0\%$
Temperature (K)	2987 ¹	$\pm 1.9\%$
Density (kgm^{-3})	0.0194 ¹	$\pm 13.8\%$
Total Enthalpy (MJkg^{-1})	8.77 ¹	$\pm 2.6\%$
Specific heat ratio	1.253 ¹	$\pm 0.2\%$
Pitot pressure (kPa)	1232	$\pm 5\%$
Mach number	7.43 ¹	$\pm 4.3\%$

¹ Quantity obtained from equilibrium chemistry solver.

The facility is instrumented with ionisation gauges and piezoelectric pressure transducers mounted along the walls of both the shock and acceleration tubes. These allow measurement of the shock speed and static wall pressure in both the shock and acceleration tubes. A piezoelectric pressure transducer was also used for measurements of the centreline Pitot pressure.

3 Force Measurement Technique

The stress wave force balance involves connecting the model to an elastic stress bar and suspending the arrangement in the test flow so that there is no restriction to movement in the flow direction (see Figure 2). With the sudden arrival of the test flow a drag force is exerted on the model causing stress waves to propagate and reflect within the model and the stress bar. These stress waves are measured and recorded using strain gauges mounted on the stress bar. The dynamic behaviour of the model/stress bar can be modelled as a linear system described by the convolution integral,

$$y(t) = \int_0^t g(t - \tau)u(\tau)d\tau \quad (1)$$

where $u(t)$ is the input to the system, $y(t)$ is the resulting output and $g(t)$ is the unit impulse response function. In experiments, the unknown drag on the model is determined from the measured output strain signal and the impulse response function. Thus, the problem is an inverse one and the drag may be found using a numerical deconvolution procedure. This technique has provided accurate force measurements on a variety of model configurations in the T4 free piston shock tunnel, located at The University of Queensland [3].

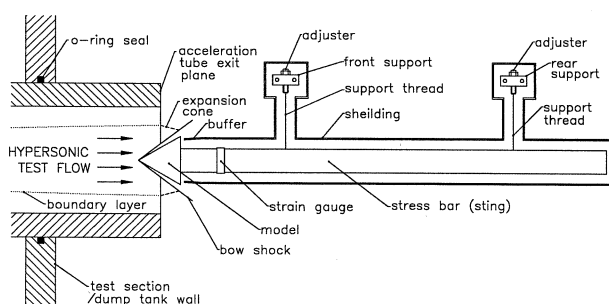


Figure 2: Schematic representation of the X1 force balance.

4 Force Balance Development

The force balance was designed to mount within the test section of the X1 facility and to support a small model within the test flow. Predictions of the test core, based upon the development of the boundary layer in the acceleration tube, indicated that the maximum model size was approximately 20 mm in diameter. The expansion cone, produced by the expanding test gas, constrained

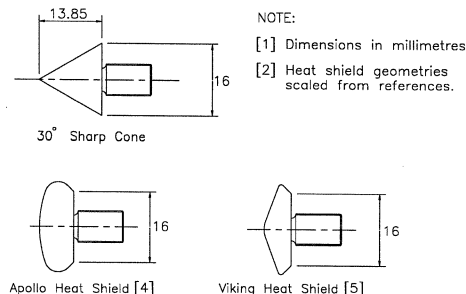


Figure 3: Model geometries used in the X1 facility.

the model geometry such that oblique bow shock reflections from the expansion cone would not impinge on the model. This was a particular concern for conical models.

Based on the above geometrical constraints, three different models were manufactured: a 30° cone, an Apollo heat shield [4] and a Viking heat shield [5] (refer to Figure 3). All of the models were made from 4140 Steel which was sufficiently robust to withstand severe test conditions. The models were threaded onto the stress bar.

The stress bar of 8 mm outside diameter, 7 mm inside diameter and 550 mm length, was instrumented with Kulite ULP semi-conductor strain gauges. The strain gauges were mounted in a half bridge (bending compensation arrangement), approximately 60 mm remote from the threaded connection to the model. This formed the basis of the force balance onto which all the different models could be attached. Brass was chosen as the stress bar material because it has a relatively low elastic wave speed (3556 ms^{-1}). This serves to increase the period before stress wave reflection from the downstream end occurs. The instrumented stress bar was then suspended in a rigid shielding and aligned so that a small gap remained between the model and the buffer (refer to Figure 2).

The dynamic responses of the three different model/stress bar arrangements were analysed using the finite element package MSC/NASTRAN. This enabled unit step responses to be obtained for a uniformly distributed pressure loading on the models. The unit step responses were then used to obtain the unit impulse response functions which were latter used in the deconvolution of the measured strain time histories.

5 Experimental Results

Experiments were conducted in two stages. The first stage involved verifying the response of the force balance to short duration tests flows. The second stage involved conducting a series of experiments to obtain drag force measurements on re-entry vehicle models.

5.1 Verification of Force Balance

The X1 facility operated in condition 1 produced a steady test flow for a period of approximately $120 \mu\text{s}$. This is illustrated in Figure 4 by a typical centre-line Pitot pressure time history.

The 30° cone was tested using this condition and drag measurements obtained through deconvolution of

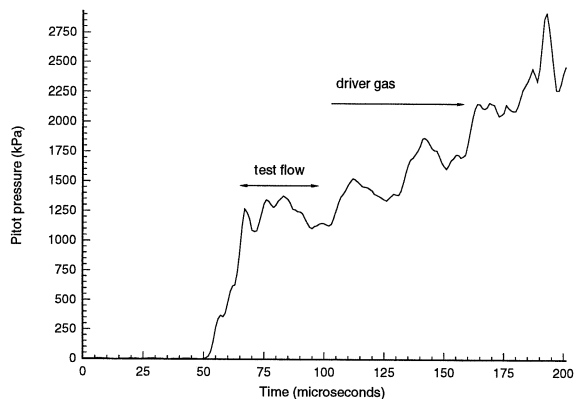


Figure 4: Typical pitot pressure time history for Condition 1.

the measured strain history, as described in section 3. The deconvolved drag measurements were then compared directly to a theoretical drag prediction. The prediction was based upon the inviscid Taylor-Maccoll [6] theory for an attached conical shock in a perfect gas. Calculations indicate that the combined effect of skin friction on the model and pressure acting in the base region (for the geometrical arrangement shown in Figure 2.) was less than 2% of the net drag on the model. A typical deconvolved drag signal obtained from the 30° cone model, along with the predicted drag force, appears in Figure 5.

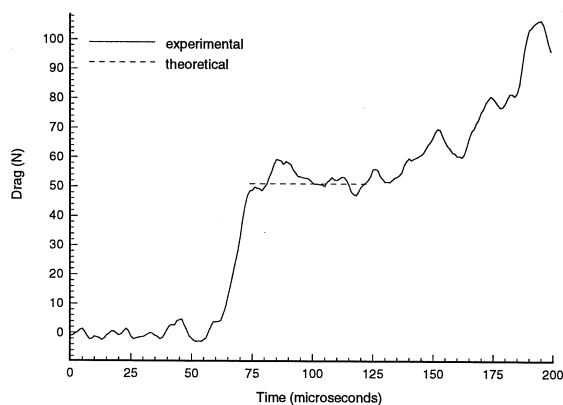


Figure 5: Comparison between measured and predicted drag force on the 30° cone model in CO₂ at M=7.4.

Figures 4 and 5 indicate that the deconvolved drag has a similar time history to the measured Pitot pressure, in that a steady drag level is measured during the period of the test flow. Note that size restrictions in the test section prevented Pitot pressure and drag measurements being obtained simultaneously. Thus zero on the time scale is arbitrary.

Agreement between predicted and experimental drag levels was found to be within 5% for repeated tests on the conical model. The difference was attributed primarily to uncertainties in the test flow conditions which corresponded to a 9% uncertainty in the measured drag.

The results from the experiments performed using Condition 1 verified that the force balance could be used to measure forces in short duration test flows.

5.2 Expansion Tube Force Measurement

The force balance was then used to obtain drag measurements on the Apollo and Viking heat shield models depicted in Figure 2. Theoretical predictions for the drag on these models were made using the finite element meshes of the models described in Section 4 and a Modified-Newtonian flow solver. An example of the finite element meshes for the Apollo heat shield used is presented in Figure 6.

Figures 7 and 8 illustrate typical deconvolved drag measurements along with theoretical predictions for the Apollo and Viking heat shield models respectively.

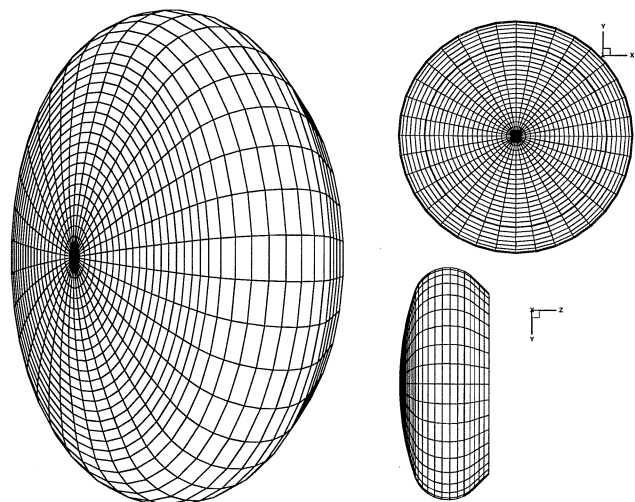


Figure 6: The finite element mesh of the Apollo heat shield used in conjunction with the Modified-Newtonian flow solver.

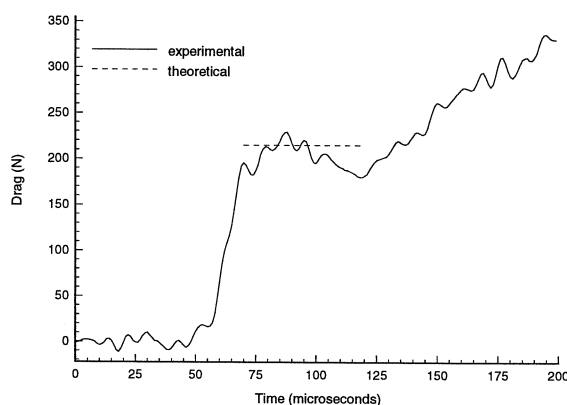


Figure 7: Comparison between measured and predicted drag force on the Viking heat shield model in CO₂ at M=7.4.

Figures 7 and 8 again indicate that the deconvolved drag history follows the pitot pressure time history. Re-

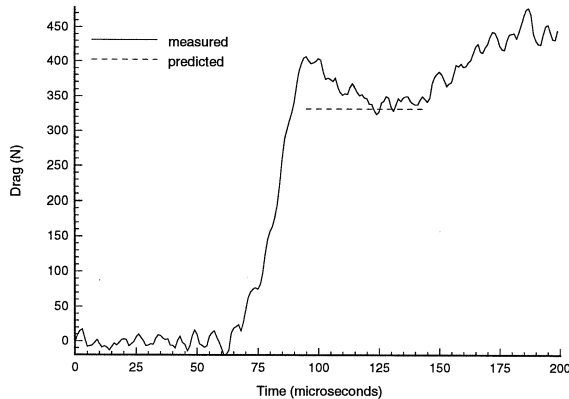


Figure 8: Comparison between measured and predicted drag force on the Apollo heat shield model in CO_2 at $M=7.4$.

peat shots on both models were used to obtain drag coefficients specific to the measured test conditions. This showed that agreement between experimental and predicted drag levels was to within within 11%. This is also consistent with the uncertainty of test conditions produced by the X1 facility and the inherent adequacies of the Modified-Newtonian flow solver. These results are summarised in Table 2.

Table 2: Comparison of Drag Coefficients

Model	$C_{D(\text{measured})}$	$C_{D(\text{predicted})}$	Difference
30° Cone	0.59	0.56	5.1%
30° Cone	0.54	0.56	3.6%
Apollo	1.61	1.76	8.5%
Apollo	1.54	1.44	6.5%
Viking	1.76	1.64	6.8%
Viking	1.86	1.66	10.8%

6 Conclusion

An extension of the force measurement technique initially proposed by Sanderson [1] has been developed for use in a free piston driven expansion tube. Preliminary tests were used to verify the response of the force balance to the short duration test flows that are typical of expansion tubes. The force balance was then used to obtain drag measurements on a variety of models, including re-entry type vehicles, in Carbon Dioxide test flows. In general, agreement between experimental and predicted drag levels was found to be within 11%.

The successful measurement of drag forces in the X1 facility extends the usefulness of short duration hypervelocity facilities, especially in the area of aerobraking and aerocapture studies. This is envisaged to be important for the development of interplanetary flight vehicles.

7 Acknowledgements

The authors gratefully acknowledge the financial support of the Australian Research Council under grant A8941305 and the use of the Modified-Newtonian flow solver de-

veloped by K. Austin at the University of Queensland, Department of Mechanical Engineering.

8 References

- [1] Sanderson S.R. and Simmons J.M. *Drag balance for hypervelocity impulse facilities*, AIAA Journal, 29(12):2185-2191, 1991.
- [2] Neely A.J., Stalker R.J. and Paull A. *High enthalpy, hypervelocity flows of air and argon in an expansion tube*, The Aeronautical Journal, 175-186, June/July 1991.
- [3] Mee D.J., Daniel W.J., Tuttle S.L. and Simmons J.M., *Balances for the measurement of multiple components of force in flows of a millisecond duration*, 19th International Symposium on Shock Waves, 26-30 July 1993 Marseille, France.
- [4] Park C., *Nonequilibrium Hypersonic aerothermodynamics*, John Wiley and Sons, Brisbane 1990.
- [5] Miller C.G., *Shock shapes on blunt bodies in hypersonic-hypervelocity helium, air and CO_2 flows, and calibration results in Langley 6-inch expansion tube.*, NASA TN D-7800, 1975.
- [6] Taylor G.I. and Maccoll J.W., *The air pressure on a cone moving at high speed*, Proc. Royal Society (London), Series A, 139:278-297, 1932.